Equation of state and pressure-induced polymorphism of $ZrSiO_4$

M. Marqués, M. Flórez, J. M. Recio, Universidad de Oviedo, E-33006 Oviedo, Spain,*

L. Gerward, Technical University of Denmark, 2800 Kongens Lyngby, Denmark,

J. Staun Olsen, Niels Bohr Institute, Oersted Laboratory, 2100 Copenhagen, Denmark

miriam@carbono.quimica.uniovi.es

Summary

In this contribution, we present the results of a combined experimental and theoretical investigation aimed to determine equation of state parameters and phase stability thermodynamic boundaries of $ZrSiO_4$ polymorphs. Experimental unit-cell data have been obtained for a powdered sample in a diamond-anvil cell using energy-dispersive synchrotron X-ray diffraction with emphasis in the pressure range 0 – 15 GPa. Total energy calculations have been performed within the density functional theory at LDA and GGA levels using a plane wave-pseudopotential scheme. Our quantum-mechanical simulations explore the two observed tetragonal structures (zircon and scheelite-type reidite) as well as other potential post-scheelite polymorphs up to 50 GPa. We find a very good agreement between our experimental and calculated pressure-volume values for the low-pressure phase of $ZrSiO_4$ in terms of the bulk modulus and linear compressibilities. Our results are discussed in relation to the discrepancies found in very recent theoretical and experimental studies. The zircon-scheelite thermodynamic phase transition is computed around 5 GPa. No other post-scheelite phase is found stable above this pressure though a decomposition into ZrO_2 (cottunite) and SiO_2 (stishovite) is predicted at about 6 GPa. These two transition pressure values are well below the experimental ranges detected in the laboratory in concordance with the large hysteresis associated with these transformations. Thermal barriers of the zircon ↔ reidite transformation are estimated from the available experimental information by coupling a Debye-like model to our static calculations. Under a martensitic perspective, we examine both a low symmetry (monoclinic) unit cell and a direct $I4_1/a$ pathway (due to the group-subgroup relationship between zircon and scheelite structures) to describe the phase transition mechanism. A preliminary evaluation of the Gibbs energy profile along these transition paths is also reported.

I. Introduction

The particular chemical and structural features of the bonding network in $ZrSiO_4$ provide a paradigmatic case to investigate the correlation between observable properties and the local geometry and interactions around the constitutive atoms of a given material. This mixed oxide presents simultaneously two nominally 4+ cations, shows the lowest compressibility for a material containing SiO_4 tetrahedra, contains interstices appropriate for hosting and retain rare-earth elements, and exhibits an anomalous and possibly unique displacive mechanism regarding silicate solid-solid transformations (Knittle and Williams 1993).

A straightforward strategy to study the chemistry and physics of the local environment of atoms in crystalline solids is the application of hydrostatic pressure. The equations of state (EOS) of the two observed polymorphs of $ZrSiO_4$, zircon and reidite, have been the subject of recent experimental and theoretical investigations. Contrarily to previous data of the zero pressure bulk modulus (B_0) for zircon around 230 GPa (Hazen and Finger 1979), van Westrenen *et al.* (2004) and Ono *et al.* (2004) obtained values around 10% lower. In addition, Ono *et al.* pointed out the non-hydrostaticity of the medium as the main reason for

the difference between their B_0 value for reidite (392±9 GPa) and the value reported by Scott *et al.* (301.4±12.5 GPa) (2002). Scott *et al.* claimed that their results in the hydrostatic regime are completely indistinguishable from the higher pressure results.

Zircon and reidite show strong structural anisotropy under temperature and pressure as manifested by the different values of their corresponding linear compressibilities, κ_a and κ_c (Finch and Hanchar 2003). The observed behavior can be summarized as follows: (i) reidite is less anisotropic than zircon, and (ii) $\kappa_a > \kappa_c$ in zircon whereas $\kappa_a < \kappa_c$ in reidite. The structural anisotropy can be traced back as due to the orientation and linkage of the constitutive polyhedra, and ultimately to the spatial localization of Si-O, Zr-O and O-O bonds. In the explanation given by Smyth *et al.* (2000) (later quoted in the review of Finch and Hanchar (2003)), we have found that Zr-O bond strengths are not correctly correlated with the observed linear compressibilities.

The last issue that has attracted our interest in this contribution is the determination of pressure and temperature ranges of stability for zircon and reidite. Static pressure (Reid and Ringwood 1969, Liu 1979, Knittle 1979, Ono *et al.* 2004, Westrenen *et al.* 2004) and shock wave compression (Kusaba *et al.* 1985, Kusaba *et al.* 1986, Leroux *et al.* 1999) experiments have identified reidite as the only high-pressure polymorph of $ZrSiO_4$. At sufficient elevated temperature and pressure, $ZrSiO_4$ is observed to decompose in SiO_2 (stishovite) and ZrO_2 (cottunite) (Tange and Takahashi 2004). Due to the high energetic barriers associated with the hysteresis of these processes, the equilibrium thermodynamic boundaries are not well constrained though positive Clapeyron *p-T* slopes for both transitions are suggested (Finch and Hanchar 2003, Tange and Takahashi 2004). Regarding mechanistic aspects of the zircon $\rightarrow$ reidite transformation, only Kusaba *et al.* (1986) have discussed two possible transition paths with special preference for a monoclinic one.

In this study, we aim to contribute to the understanding of the structural and stability behavior of $ZrSiO_4$ under hydrostatic pressure. Diamond-anvil cell experiments using energy-dispersive synchrotron X-ray diffraction in powdered samples and static total energy calculations based on the density functional approximation were carried out in a pressure range up to around 15 GPa and 50 GPa, respectively. This combined experimental and theoretical investigation allows to clarify some of the discrepancies found in previous works. In particular, we report and analyze in detail the EOS of zircon and reidite in terms of bulk and linear compressibilities with a special emphasis in the comparison with other experimental data. The second objective of our study is the characterization of zircon $\rightarrow$ reidite and reidite $\rightarrow$ SiO_2 (stishovite) + ZrO_2 (cottunite) transformations. Associated transition properties are evaluated and the effects of temperature on the equilibrium thermodynamic boundaries are discussed. Preliminary analysis of the two transition paths proposed by Kusaba *et al.* (1986) are also reported.

The paper is organized in four more sections. Next, a brief description of the experimental and computational procedures is given. Section III contains zero pressure structural results and the analysis of the EOS parameters of zircon and reidite. Phase transition properties and stability ranges of $ZrSiO_4$ polymorphs are presented in Section IV. The paper ends with the main conclusions of our work.

II. Experimental methods and Computational details

II.A. Experimental methods

High-pressure powder x-ray diffraction patterns were recorded at room temperature using the white-beam method and synchrotron radiation at Station F3 of HASYLAB-DESY in Hamburg, Germany. The diffractometer, working in the energy-dispersive mode, has been described elsewhere (Olsen 1992). High pressures were obtained in a Syassen-Holzapfel type

diamond-anvil cell. A finely ground powder sample and a ruby chip were placed in a 200 μm diameter hole in an inconel gasket, pre-indented to a thickness of 60 μm. A 16:3:1 methanol:ethanol:water mixture was used as the pressure-transmitting medium. The pressure in the cell was determined by measuring the wavelength shift of the ruby R_1 luminescence line and applying the non-linear pressure scale of Mao *et al.* (1986). The Bragg angle of each run was calculated from a zero-pressure spectrum of sodium chloride in the diamond-anvil cell.

Synchrotron x-ray diffraction (XRD) spectra for zircon were recorded at various pressures. From each spectrum, values for the lattice parameters and the unit-cell volume can be derived and refined. The pressure-volume data were then described by the Birch-Murnaghan equation of state (Birch 1947):

$$P = \frac{3}{2} B_0 (x^{-7/3} - x^{-5/3})[1 - \frac{3}{4}(4 - B_0^{'})(x^{-2/3} - 1)], \quad (1)$$

where $x = V/V_0$, V being the volume at pressure p, and V_0 the volume at zero pressure, B_0 is the bulk modulus and B_0' its pressure derivative, both parameters evaluated at zero pressure. Values of B_0 and B_0' were obtained from a least-squares fit of Equation (1) to the experimental data points.

II.B. Computational details

Total energy calculations at selected unit cell volumes of zircon, reidite, stishovite (SiO_2), and cottunite (ZrO_2) structures were performed under the framework of the density functional theory as implemented in the VASP package (Kresse and Furthmuller 1996). Results at the local density approximation (LDA) and generalized gradient approximation (GGA) levels are presented. We follow a rather standard planewave-pseudopotential scheme with other computational parameters (energy cutoffs, *k*-space grids, etc.) assuring convergence and accuracy in the optimization of the unit cell geometry of the corresponding polymorphs.

In a second step, we convert the calculated energy-volume points (E_i,V_i) into static (zero temperature and zero point vibrational contributions neglected) and finite temperature pressure-volume (p_i,V_i) isotherms using numerical and analytical procedures coded in the GIBBS program (Blanco *et al.* 2004). Thermal contributions are included by means of a non-empirical quasi-harmonic Debye-like model that only needs the set of (E_i,V_i) points and the calculated static bulk modulus to evaluate thermodynamic properties at different temperatures. Due to the approximate character of the Debye model, we mainly focus on the static results, though the effect of temperature will be also considered in the discussion of the transformation equilibrium boundaries. The main outcome of our simulation strategy is the pressure dependence (from 0 up to 50 GPa) of all the unit cell parameters, atomic coordinates, and Gibbs energies (G) of the $ZrSiO_4$, SiO_2, and ZrO_2 structures.

III. Structural properties and equation of state parameters

Zircon and reidite belong, respectively, to the $I4_1/amd$ and $I4_1/a$ space groups. Their conventional unit cells are tetragonal and contain four Zr and Si atoms at special positions, and sixteen O atoms at (0,y_z,z_z) and (x_r,y_r,z_r), respectively. Both structures have been described in detail previously (see for example Finch and Hanchar 2003 and Tennant *et al.* 2004, and references therein). Our experimental and calculated lattice parameters a and c and oxygen coordinates (u,v,w) are collected in Table 1 along with other representative experimental data. We found a good agreement between previous and present results. Notice that the expected underestimation of the structural parameters at the LDA level is only within 1%, whereas GGA overestimates up to 4% the geometry of $ZrSiO_4$ polymorphs.

Table 1. Summary of zero pressure cohesive properties and equation of state parameters of zircon and reidite. *a* and *c* in Å, V_0 is the volume per formula unit in Å^3 and B_0 in GPa.

	ZIRCON					REIDITE			
a	6.6042[a]	6.6058[b]	6.601[c]	6.599[d]	6.704[e]	4.734[f]		4.723[d]	4.788[e]
c	5.9796[a]	5.9772[b]	5.975[c]	5.959[d]	6.040[e]	10.510[f]		10.411[d]	10.640[e]
u						0.28[f]		0.2585[d]	0.2584[e]
v	0.0660[a]			0.0661[d]	0.0667[e]	0.14[f]		0.1573[d]	0.1571[e]
w	0.1951[a]			0.1944[d]	0.1953[e]	0.07[f]		0.0788[d]	0.0774[e]
V_0	65.20[a]	65.20[b]	65.10[c]	64.87[d]	67.86[e]	58.88[f]	57.78[g]	58.06[d]	60.97[e]
B_0	227[a]	201[b]	225±8[c]	231[d]	201[e]		392±9[g]	258[d]	221[e]
B_0'	6.5[a]	3.9[b]	6.5±1.6[c]	4.8[d]	5.1[e]		4[g]	4.5[d]	5.0[e]

[a]Experimental. $ZrSiO_4$ nonmetamict natural (Hazen and Finger 1979).
[b]Experimental. $ZrSiO_4$ synthetic pure (van Westrenen *et al.* 2004).
[c]Experimental. $ZrSiO_4$ synthetic pure (98%). This work.
[d]Calculated. LDA. This work.
[e]Calculated. GGA. This work.
[f]Experimental. Shock wave (Kusaba *et al.* 1986).
[g]Experimental. Static (Ono *et al.* 2004).

According to the experimental data reported by Hazen and Finger (1979), Ozkan *et al.* (1978), and Rios *et al.* (2003), the room temperature (RT) value of B_0 in zircon lays within a range of 225-230 GPa. Similar or higher values have been obtained using several computational techniques (Crocombette *et al.* 1998, Akhtar *et al.* 2003, Fleche 2002, Farnan *et al.* 2003, and Devanathan *et al.* 2004). The evaluation of B_0 from the elastic constants experimentally determined by Ozkan *et al.* (1974) gives also a value of 225.2 GPa. We refer to the data from all these works as set I. In set II, we include recent investigations of the compressibility of zircon in diamond anvil cells using X-ray diffraction techniques. In these experiments, van Westerenen *et al.* (2004) and Ono *et al.* (2004) have obtained, respectively, 199±1 GPa and 205±8 GPa for B_0 at RT. In addition, GGA calculations of Farnan *et al.* (2003) yield only a slightly lower value of 196 GPa. It should be pointed out that the effect of fixed or variable B_0' parameters does not explain the existence of these two sets of B_0 around 225 GPa and 200 GPa, respectively,

The origin of such discrepancies is analyzed in detail by van Westrenen *et al.* (2004) listing a number of factors affecting the experimental determination of EOS parameters in the zircon structure of $ZrSiO_4$: (i) use of different techniques and analytical procedures lead to systematic differences around 5%, (ii) short pressure ranges covered by the measurements provide less precise data, (iii) presence of impurities (as in many natural samples) increases unit cell volumes and decreases B_0, and (iv) radiation damage (metamict zircon) produces amorphous domains and also reduces the bulk modulus. Nevertheless, using the above arguments a clear conclusion can not be drawn to explain the existing discrepancies, and a combination of effects is proposed (van Westrenen *et al.* 2004).

Our pressure-normalized volume diagram plotted in Fig. 1 (V_0 is the corresponding zero pressure volume of zircon) illustrates quantitatively the observed differences in the response of the unit cell volume of zircon to hydrostatic pressure. It is apparent the very good agreement between our experimental and calculated LDA (p_i,V_i) values, both yielding B_0 around 230 GPa, and therefore supporting the data of set I. In the low-pressure range covered by the experiments of Ono *et al*., the deviations from our experimental results are almost negligible, indicating that the error bars of the corresponding B_0 values should be taken into consideration. It should be also emphasized that V_0 is used as a free parameter in the EOS fitting of Ono *et al.* This procedure yields a slightly higher value (65.35 Å^3) than the one obtained directly in the X-ray diffraction experiments (65.25 Å^3) and tends to lower the

final B_0 parameter. Larger discrepancies appear at increasing pressures with respect to the experimental values of van Westrenen *et al.* (2004) as expected from the two different values of B_0. Honestly speaking, we might remark that our GGA results, also plotted in Fig. 1, are in fair agreement with the measured points of van Westrenen *et al.* and yield a B_0 value close to the data of set II. Nevertheless, we are more confident with our LDA calculations since they provide an accurate overall description of the structure, the compressibility and the phase transition properties of $ZrSiO_4$. Results at LDA level of computation have been also reported in our previous work on group-IV nitrides (Marqués *et al.* 2004) using the same VASP methodology.

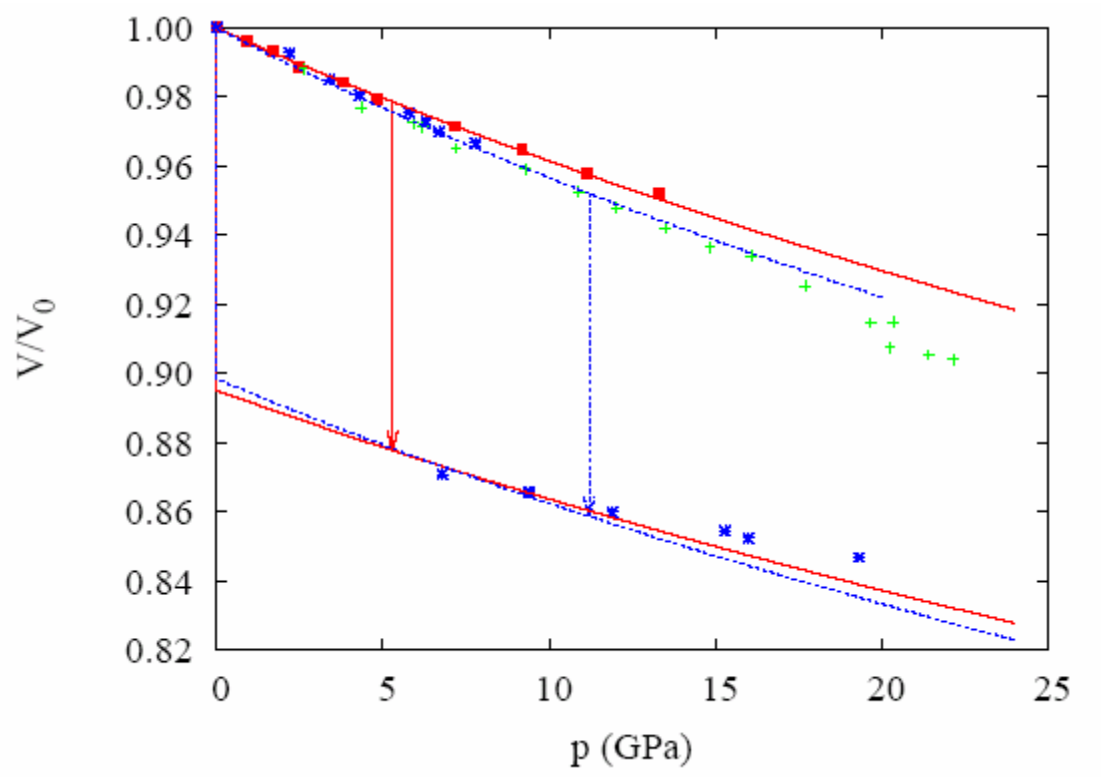

Fig. 1. Normalized volume versus pressure diagram. Symbols stand for the experimental data of this work (red solid squares), van Westrenen *et al.* 2004 (green crosses), and Ono *et al.* 2004 (blue stars). Lines are our calculated data under the LDA (red solid) and GGA (blue dashed) approximations. Arrows represent calculated volume collapses at the zircon → reidite transition (see Section IV).

For reidite, the difference between the two experimental values of B_0 (392±9, Ono *et al.* 2004, and 301.4±12.5, Scott *et al.* 2002) is as large as around 100 GPa. These two values are much higher than our computed values. GGA results produce definitively a too compressible scheelite-type polymorph, whereas our LDA value is around 14% lower than the value reported by Scott *et al.*. The particular (p_i,V_i/V_0) data points of Ono *et al.* do not show, however, large discrepancies with respect to our calculated values. Differences come from the rate these points decrease as pressure is applied. Notice that, again, Ono *et al.* zero pressure volume of reidite is not directly obtained in their experiments, but determined in the EOS fitting procedure. Their value is now almost 2% lower than previous experimental data of Reid and Ringwood (1969) and Kusaba *et al.* (1986) which might be considered a factor to overestimate B_0.

Previous and present results evidence the structural anisotropy of the two $ZrSiO_4$ polymorphs. It can be measured in terms of observable properties as the linear

compressibilities along *a* and *c* axes, κ_a and κ_c, respectively. Again, opposite results are obtained for zircon and reidite (see Fig. 2). In agreement with the experimental data, *a* is more (less) compressible than *c* in zircon (reidite), and the degree of structural anisotropy under pressure of zircon is greater than that of reidite. Our calculated values for zircon (κ_a =1.68x10^{-3} GPa^{-1}, κ_c = 0.98x10^{-3} GPa^{-1}) are similar to the linear compressibilities determined by Hazen and Finger (1979) (κ_a =1.6x10^{-3} GPa^{-1}, κ_c = 0.95x10^{-3} GPa^{-1}). Chains of edge linked ZrO_4 and SiO_4 tetrahedra parallel to the *c* axis are the responsible of the low compressibility along this axis in zircon. In reidite, calculated values (κ_a = 1.10x10^{-3} GPa^{-1}, κ_c = 1.69x10^{-3} GPa^{-1}) show greater discrepancies with the values reported by Scott *et al.* (2002) (κ_a = 0.742x10^{-3} GPa^{-1}, κ_c = 1.08x10^{-3} GPa^{-1}), though it is to be noted that their values do not recover the value they reported for the bulk ($\kappa = 2\kappa_a + \kappa_c$). As pointed out by these authors, the low compressibility along the *a* axis in reidite has to be related to the repulsions between oxygen atoms whose shortest interatomic distances are found in the *ab* plane.

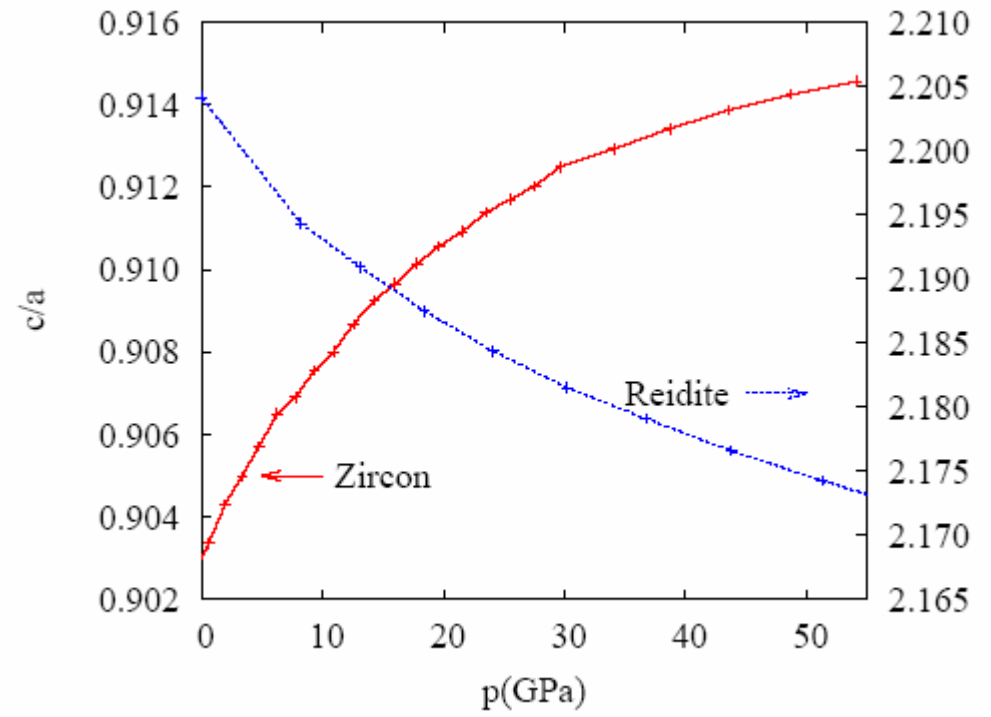

Fig.2 Pressure effects on the c/a ratio of zircon and reidite polymorphs according to our LDA calculations.

IV. Stability and phase transition properties

$ZrSiO_4$ is known to display a pressure-induced first order phase transition from zircon to reidite. At elevated temperatures, $ZrSiO_4$ decomposes into its simple oxides, very likely β-crystoballite SiO_2 and tetragonal ZrO_2 at zero pressure (Mursic *et al.* 1992), or stishovite SiO_2 and cottunite-type ZrO_2 at high-pressure (Tange and Takahashi 2004). There is a good deal of experimental data (Reid and Ringwood 1969, Liu 1979, Kusaba *et al.* 1985, Kusaba *et al.* 1986, Mursic *et al.* 1992, Knittle and Williams 1993, Leroux *et al.* 1999, Glass *et al.* 2002, Finch and Hanchar 2003, Westrenen *et al.* 2004, Ono *et al.* 2004, Tange and Takahashi 2004) concerning both thermodynamic and mechanistic aspects of these transformations, and less information from the theoretical side (Crocombette *et al.* 1998, Farnan *et al.* 2003) The experimental facts associated with the stability of zircon and reidite polymorphs can be summarized as follows: (i) Volume collapse is around 10-11% for zircon $\rightarrow$ reidite phase transition, (ii) Static experiments show that this transformation is observed at pressures in the range of 10-15 GPa when temperature is increased up to 1000-1500 K (Ono *et al.* 2004, Reid and Ringwood 1969, Liu 1979), whereas at room temperature the transition is also

possible if pressure is increased up to approximately 20-23 GPa (Knittle and Williams 1993, van Westrenen *et al.* 2004), (iii) shock wave studies found this transformation to occur very fast (microsecond time scale), and at much higher pressures (30-50 GPa) (Kusaba *et al.* 1985, Kusaba *et al.* 1986, Leroux *et al.* 1999), (iv) zircon $\rightarrow$ reidite transformation exhibits large hysteresis, zircon is not recoverable from reidite at zero pressure unless heated up to 1273 K (Kusaba *et al.* 1985), and (v) the thermodynamic boundary of the high-pressure decomposition of $ZrSiO_4$ presents a positive Clapeyron slope (Tange and Takahashi 2004).

To discuss theoretical results in relation to the above experimental data we should bear in mind the difference between our calculated thermodynamic (equilibrium) transition pressures (p_t) and the experimental ones (p_{exp}). That the zircon $\rightarrow$ reidite and $ZrSiO_4 \rightarrow ZrO_2 + SiO_2$ transformations are kinetically hindered is obvious from the experimental data collected so far. Thus, when the parent and product phases are close to equilibrium, the energetic barriers associated with these transformations can be overcome only at sufficient high temperatures, and then observed transition pressures may be compared with thermodynamic transition pressures. It is reasonable to accept that the barrier heights for the direct and inverse transformations depend strongly on pressure but are negligibly affected by temperature. In this way, we may estimate the thermal energy in the 1000-1500 K range as the activation barrier for the equilibrium zircon $\leftrightarrow$ reidite transition (Liu 1979, Ono *et al.* 2004), whereas for the reidite $\leftrightarrow ZrO_2 + SiO_2$ decomposition the corresponding value is below 1800 K (Tange and Takahashi 2004).

The validity of this analysis is illustrated by comparing the equilibrium boundary of this transition with the experimental zircon $\rightarrow$ reidite transition pressures of Knittle and Williams (23 GPa) (Knittle and Williams 1993) and van Westrenen *et al.* (19.7 GPa) (van Westrenen *et al.* 2004) obtained at 300 K. From the high temperature data, and assuming a positive Clapeyron slope for this transformation (Knittle and Williams 1993, Finch and Hanchar 2003), p_t is expected to be below 10 GPa at room temperature. Our static value of around 5.3 GPa (see Fig. 3) is in concordance with this expectation and is also in good agreement with the calculated values of Crocombette and Ghaleb (1998) and Farnan *et al.* (2003). The overpressure needed to observe the zircon $\rightarrow$ reidite transformation at 300 K implies that the activation energy for the direct transformation has decreased with compression (Knittle and Williams 1993) in such a way that the thermal energy at 300 K is enough to overcome the barrier. Similarly, the reidite $\rightarrow$ zircon transformation detected at zero pressure after heating up to 1273 K informs on the barrier height for the inverse transformation at this pressure.

A good estimation of such barrier heights is obtained by coupling the Debye model implemented in the GIBBS code (Blanco *et al.* 2004) to our static total energy calculations. We have found a good agreement between the results of several thermodynamic properties obtained within this model and those obtained by Fleche (2002) in zircon using a more sophisticated procedure that involves explicit evaluation of Γ-point vibrational frequencies. At their corresponding static equilibrium unit cells, Debye's temperatures (Θ_D) are computed for zircon (Θ_D^z = 795.8 K) and reidite (Θ_D^r = 823.3 K). The available vibrational energy for zircon at 300 K and 23 GPa evaluated within our Debye model is 64.87 kJ/mol, whereas for reidite at p = 0 and 1273 K is 193.78 kJ/mol. Since we are interested in the static barriers, i.e. the difference between the static Gibbs energy of zircon (or reidite) and the static Gibbs energy of the transition state, $G^{\ddagger}$, we substract to these values the corresponding zero point energies, 53.13 kJ/mol for zircon at 23 GPa and 46.16 kJ/mol for reidite at zero pressure. Assuming a linear dependence of $G^{\ddagger}$ with pressure (as approximately G_{zircon} and $G_{reidite}$ show), the thermal barrier at p_t can be evaluated (see Fig. 3). The value estimated amounts 132.59 kJ/mol which is equivalent (using either the vibrational energy of zircon or reidite corrected with the corresponding zero point energy) to a temperature of around 1200 K, in the range of Ono *et al.* (2004) experiments.

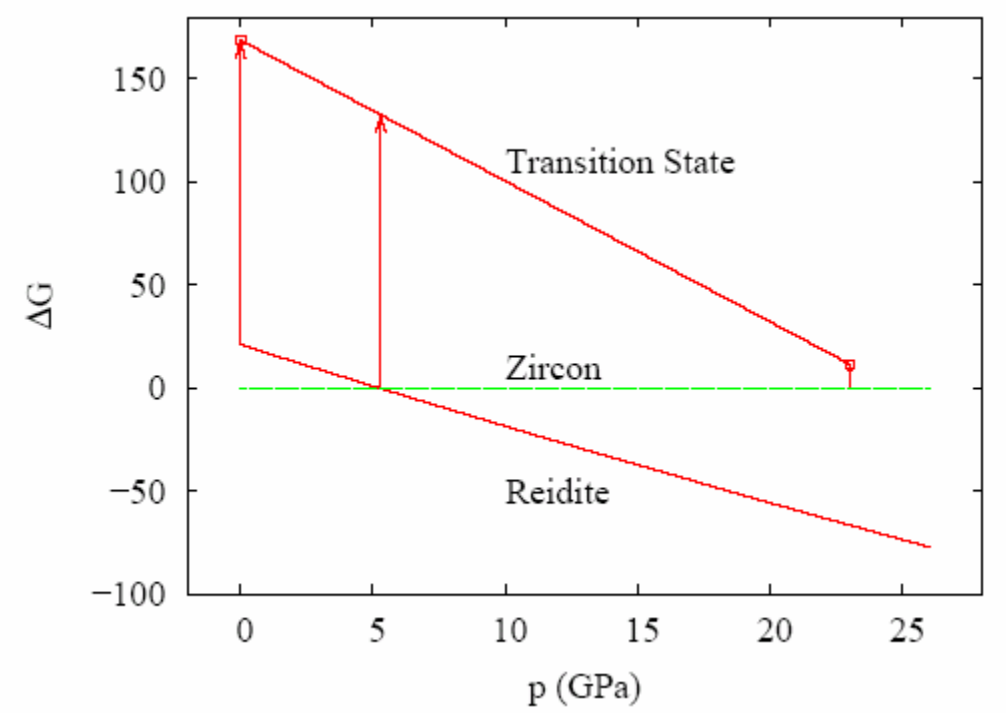

Fig. 3 Pressure dependence of the Gibbs energy (kJ/mol) of reidite relative to zircon according to present LDA calculations. Thermal barriers at 0 GPa (reidite → zircon), p_t, and 23 GPa (zircon → reidite) denoted by arrows and calculated using also our Debye model.

As regards the thermodynamic properties related to the stability of the two polymorphs, we have obtained a decrease in the unit cell volume of $ZrSiO_4$ of 10.3% at the transition pressure of the zircon → reidite transformation (see red arrow in Fig. 1), and around 8.9% for the $ZrSiO_4$ (reidite) → ZrO_2 (cottunite-type) + SiO_2 (stishovite) decomposition whose equilibrium pressure is computed at 6.3 GPa according to our static LDA calculations. Both transformations exhibit an increase of *B* at the corresponding transition pressures which can be explained as mainly due to the volume reduction.

We have also explored the effect of temperature in the equilibrium pressure boundaries of these two transformations. The inclusion of vibrational energy and entropy contributions into static results was again performed with the Debye model. We have found a qualitatively satisfactory picture with both Clapeyron slopes slightly positive in the temperature ranges covered by our calculations. This means that there is a small decrease of entropy associated to these transitions, supporting the analysis of Finch and Hanchar in zircon. p_t increases 1.9 GPa from 0 to 1800 K for zircon → reidite transformation, whereas in the $ZrSiO_4$ (reidite) → ZrO_2 (cottunite-type) + SiO_2 (stishovite) transformation the increment in p_t is 1.5 GPa in the range 0-1400 K. Though, the absolute values of the transition pressures are slightly below the experimental ones, the overall description is very reasonable.

The study of post-scheelite phases have been performed by computing the fergusonite and wolframite structures. In the pressure range covered in our calculations, all the geometrical optimizations carried out in the fergusonite-type structure (*I2/a*) revert back to the scheelite-type lattice in concordance with their subgroup-group relationship. On the other hand, the total energy-volume curve of the wolframite structure shows a minimum at V_0 = 56.71 Å^3 and around 50 kJ/mol higher in energy than that of the reidite structure at zero pressure. An hypothetical reidite → wolframite transition is predicted at pressures above 50 GPa well beyond the decomposition of $ZrSiO_4$ into its simple oxides.

Finally, preliminary results of our analysis of the zircon → reidite transition mechanism are presented. The two pathways suggested by Kusaba *et al.* (1986) have been considered at

the calculated transition pressure. On the one hand, we have used the reidite $I4_1/a$ space group, which also allows to describe the zircon structure keeping the same lattice parameters as in its conventional $I4_1/amd$ space group, but with new Zr, Si, and O positions at (0, 0.25,0.125), (0,0.25,0.625), and (0,0.5653,0.1946), respectively. As a first approximation, we choose the *c/a* ratio as the transformation coordinate evolving from 0.9059 (zircon) to 2.1990 (reidite). The evaluation of the Gibbs energy profile has been performed under different schemes including linear interpolations of lattice parameters and oxygen coordinates. This strategy yields unphysical large activation barriers of about 1540 kJ/mol. If the oxygen coordinates are optimized along the transition path, then the activation barrier is decreased down to 236 kJ/mol. On the other hand, Kusaba *et al.* (1986) proposed a monoclinic cell to connect zircon and reidite structures. The cell angles are 90° and 114.5° for zircon and reidite, respectively, at p_t. The cell parameters changes from $a = c = 6.545$ Å, $b = 5.929$ Å in zircon to $a = c = 6.139$ Å, $b = 6.641$ Å in reidite. The atomic coordinates of Zr and Si have the same values in zircon and reidite and are fixed in the calculations. We choose the cell angle β as the transformation coordinate and linearize the unit cell parameters but optimize the oxygen coordinates along the transition path. This scheme produces an energy profile with a transition state only 111 kJ/mol above the zircon and reidite structures, very close to the activation barrier estimated from our precedent analysis. Therefore, this monoclinic pathway appears as the most probable one. Further improvements are being carried out by considering the optimization of the rest of the unit cell parameters.

V. Conclusions

We presented a combined theoretical and experimental analysis of the structure and stability of $ZrSiO_4$ under hydrostatic pressure, with emphasis in the zircon ↔ reidite phase transition. Our LDA calculations provide an accurate overall description of the behavior of this system (more accurate than the GGA ones). Both, our LDA calculations and our diamond-anvil cell experiments, give a B_0 value for zircon around 230 GPa, thus supporting the experimental and theoretical results included in the set I discussed above. Since recent static compression data yield B_0 values around 10% lower, we suggest that ultrasonic measurements on synthetic pure zircon were performed in order to determine elastic constants and bulk modulus. Our LDA value of B_0 for reidite (258 GPa) is about 14% smaller than the value reported by Scott *et al*. (2002) and much smaller than that obtained by Ono *et al.* (2004) (around 400 GPa). In agreement with the available experimental information, the degree of structural anisotropy under pressure obtained for zircon is greater than that of reidite, the linear compressibility of the former along the *a* (*c*) axis being greater (smaller) than that along *c* (*a*). We also analyzed the consistency of the experimental information available for the zircon ↔ reidite transformation and estimated the thermal barriers for it by coupling a Debye-like model to our static calculations (133 kJ/mol at the thermodynamic boundary).. The calculated static equilibrium transition pressure for this transformation (5.3 GPa) agrees reasonably with the equilibrium experimental value inferred at room conditions from the high temperature experimental data. The activation barrier estimated from our LDA calculations on a monoclinic transition path (111 kJ/mol) is slightly lower than that obtained from the analysis of the experimental data.

Acknowledgments

Financial support from the Spanish DGICYT, Project No. BQU2003-0466, is gratefully acknowledged by M.M., M.F., and J.M.R. Part of this work was performed during the stay of J.M.R. at the Laboratoire de Chimie Physique (Université Pierre et Marie Curie, Paris) under the project HPC-EUROPA (RII3-CT-2003-506079). We thank HASYLAB-DESY for permission to use the synchrotron radiation facility. L.G. and J.S.O. acknowledge financial support from the Danish Natural Sciences Research Council through DANSYNC.

REFERENCES

AKHTAR M. J. AND WASEEM S., 2003. *Solid State Sciences*, 5, 541-548.
BIRCH, F. J., 1947. *Phys. Rev.*, 71, 809-824.
BLANCO M. A., FRANCISCO E., AND LUAÑA V, 2004. *Comput. Phys. Commun.*, 158, 57-72.
CALATAYUD M., MORI-SÁNCHEZ P., BELTRÁN A., MARTÍN PENDÁS A., FRANCISCO E., ANDRÉS J., AND RECIO J. M., 2001. *Phys. Rev. B,* 64, 184113-1-9.
CROCOMBETTE J. P. AND GHALEB D., 1998. *J. Nuclear Mater.*, 257, 282-286.
DEVANATHAN R., CORRALES L. R., WEBER W. J., CHARTIER A., AND MEIS C., 2004. *Phys. Rev. B*, 69, 064115-1-9.
FARNAN I., BALAN E., PICKARD C. J., AND MAURI F., 2003. *Amer. Miner.*, 88, 1663-1667.
FINCH R. J. AND HANCHAR J. M., 2003. Structure and Chemistry of Zircon and Zircon-Group Minerals. *In* HANCHAR J. M. AND HOSKIN P. W. O. eds. Zircon. (Mineralogical Society of America, Washington, D.C.), *Reviews of Mineralogy and Geochemistry*, 53, 1-25.
FLECHE J. L., 2002. *Phys. Rev. B,* 65, 245116-1-10.
GLASS B. P., LIU S., AND LEAVENS P. B., 2002. *Amer. Miner.,* 87, 562-565.
GRACIA L., BELTRÁN A., ANDRÉS J., FRANCO R., AND RECIO J. M., 2002. *Phys. Rev. B,* 66, 224114-1-7.
HAZEN R. M. AND FINGER L. W., 1979. *Amer. Miner.*, 64, 196-201.
KNITTLE E. AND WILLIAMS Q., 1993. *Amer. Miner.*,78, 245-252.
KRESSE G. AND FURTHMULLER J., 1996. *Phys. Rev. B*, 54, 11169-11186.
KUSABA K., SYONO Y., KIKUCHI M., AND FUKUOKA K, 1985. *Earth Planet. Sci. Lett.*, 72, 433-439.
KUSABA K., YAGI T., KIKUCHI M., AND SYONO Y., 1986. *J. Phys. Chem. Solids,* 47, 675-679.
LEROUX H., REIMOLD W. U., KOEBERL C. , HORNEMANN U., AND DOUKHAN J.-C., 1999. *Earth Planet. Sci. Lett.,* 169, 291-301.
LIU L.-G., 1979. *Earth Planet. Sci. Lett.*, 44, 390-396.
MAO H. K., XU J., AND BELL P. M., 1986. *J. Geophys. Res.*, 91, 4673.
MARQUÉS M., OSORIO J., AHUJA R., FLÓREZ M., AND RECIO J. M., 2004. *Phys. Rev. B*, 70, 104114-1-11.
MURSIC Z., VOGT T., AND FREY F., 1992. *Acta Cryst. B*, 48, 584-590.
OLSEN J.S., 1992. *Rev. Sci. Instrum.*, 83, 1058.
ONO S., TANGE Y., KATAYAMA I., AND KIKEGAWA T., 2004. *Amer. Miner.*, 89, 185-188.
OZKAN H., CARTZ L., AND JAMIESON J. C., 1974. *J. Appl. Phys.*, 45, 556-562.
OZKAN H., 1978. *Phys. Chem. Miner.*, 2, 215.
RECIO J. M., FRANCO R., MARTÍN PENDÁS A., BLANCO M. A., AND PUEYO L., 2001. *Phys. Rev. B*, 63, 184101-1-7.
REID A. F. AND RINGWOOD A. E., 1969. *Earth Planet. Sci. Lett.*, 6, 205-208.
RIOS S. AND BOFFA-BALLARAN T., 2003. *J. Appl. Cryst.*, 36, 1006-1012.
ROBINSON K., GIBBS G. V., AND RIBE P. H., 1971. *Science*, 172, 567-570.
ROBINSON K., GIBBS G. V., AND RIBE P. H., 1971. *Amer. Miner.*, 56, 782-790.
SCOTT H. P., WILLIAMS Q., AND KNITTLE E., 2002. *Phys. Rev. Lett.,* 88, 015506-1-4.
SMYTH J. R., JACOBSEN S. D., AND HAZEN R. M., 2000. Comparative Crystal Chemistry of Orthosilicate Minerals. *In* HAZEN R. M. AND DOWNS R. T. eds. High-Temperature and High-Pressure Crystal Chemistry. (Mineralogical Society of America, Washington, D.C.), *Reviews of Mineralogy and Geochemistry,* 41, 202-209.
TANGE Y., AND TAKAHASHI E., 2004. *Phys. Earth Planet. Interiors*, 143, 223-229.
TENNANT W. C., CLARIDGE R. F. C., WALSBY C. J., AND LEES N. S., 2004. *Phys. Chem. Miner.*, 31, 203.
WANG X., LOA I., SYASSEN K., HANFLAND M., AND FERRAND B., 2004. *Phys. Rev. B*, 70, 064109-1-6.
van WESTRENEN W., FRANK M. R., HANCHAR J. M., FEI Y., FINCH R. J., AND ZHA C.-S., 2004. *Amer. Miner.*, 89, 197-203.